Experimental Subsonic Drag Properties of the Space Shuttle Orbiter TPS Tiles

D.J. Norton*
Texas A&M University, College Station, Texas
and
R.E. White†
General Dynamics Co., Ft. Worth, Texas

The drag characteristics of the space shuttle orbiter thermal protection system (TPS) tiles were studied experimentally in subsonic flow. Full-scale tiles were mounted to a 3.05×3.5 m test board in four configurations plus a completely smooth case. Pressure gradients were produced by tilting the board relative to the freestream. The drags due to steps, slots, and gaps between the tiles were evaluated at various orientations, pressure gradients, and Reynolds numbers. Results showed that the contribution of gaps and slots were minor compared to those of typical steps. The results for skin friction did not correlate as a fully rough surface. Thus, the surface area of the TPS tiles was sufficient to allow smooth-wall Reynolds number effects even though the steps between tiles could double the skin friction.

Nomenclature

A,C,D = constants in log-law
a = width of a tile element
C_D = independent drag coefficient
C_f = local skin friction coefficient
C_p = pressure coefficient
E,F,G = constants in the power-law formulation
d,e = gap depth and width
H = shape factor, θ/δ^*
k = step height
L = test plate length
N = number of roughness elements
n = power-law exponent
p = static pressure
q = dynamic pressure $= \rho u^2/2$
Re = Reynolds number
u = local, time-averaged velocity
u^* = friction velocity $= \sqrt{\tau_o/\rho}$
ΔU_I = roughness velocity shift
x,y = axial, normal coordinates
α = angle of attack
δ = boundary-layer thickness
δ^* = displacement thickness
θ = momentum thickness
λ = repeat interval of roughness element
ρ = density
ν = kinematic viscosity

Subscripts and Superscripts

e = edge of the boundary layer
eff = effective
i = pertaining to the ith roughness element
L = length
k = step height
o = wall, origin
R = rough
S = smooth
$'$ = referenced to virtual origin
$-$ = average
∞ = freestream

Received July 6, 1976; revision recieved Oct. 20, 1976
Index category: Boundary Layer and Convective Heat Transfer—Turbulent.

*Associate Professor, Aerospace Engineering. Member AIAA.
†Senior Aerodynamic Engineer. Member AIAA.

Introduction

TO achieve the difficult re-entry phase of the space shuttle mission, large areas of the orbiter are covered with tiles bonded to the outer skin. The tiles are 152.4×152.4 mm in area and between 19.0 and 51.2 mm thick. The tiles are made of a lightweight insulating material with a ceramic coating. Although the tiles are quite resistant to thermal loads, mechanical loads caused by expansion must be avoided. Therefore, each tile is separated from adjacent tiles by a distance of 1.28 mm to allow for expansion (gaps). Figure 1 presents a schematic of the layup of the tiles on the surface. Since the tiles are flat and the vehicle surfaces are curved, there can be height mismatch between adjoining tiles (steps).

In this paper, experimental work dealing with tile roughness elements is presented. This work covers experimental, subsonic, flat-plate and pressure gradient data for 5 different configurations ranging from aerodynamically smooth up to tiles with 3.2 mm steps and 1.6 mm gaps between tiles.

Since the space shuttle orbiter is unpowered after the deorbit manuever, the lift-to-drag ratio determines the cross range flexibility in reaching the landing site and it controls the sink speed prior to flare. The lift characteristics are determined adequately by model tests as are certain drag terms (base drag, forebody drag, miscellaneous terms). However, the skin friction, including TPS drag, is more Reynolds-number sensitive at the lower Reynolds numbers, and skin friction coefficients are larger. The vehicle enters subsonic flow at about 20 km at which point the smooth skin friction drag is about 15% of the total. Adding in TPS drag effects may cause a 50% variation in the skin friction drag. The purpose of this study was to obtain drag data for typical tile configurations, and to determine the effects of Reynolds number and pressure gradients.

Experiment

In order to simulate, as closely as possible the flow and roughness conditions expected to occur on the orbiter, an experiment was designed to permit large Reynolds numbers in the Texas A&M 7×10 ft low-speed wind tunnel. The experimental apparatus consisted of a plate 3.05 m in width with seals at the tunnel walls and was pivoted about the center so that the angle of attack relative to the upstream flow direction could be varied. Varying the angle of attack permitted the study of pressure gradient effects on the boundary layer.

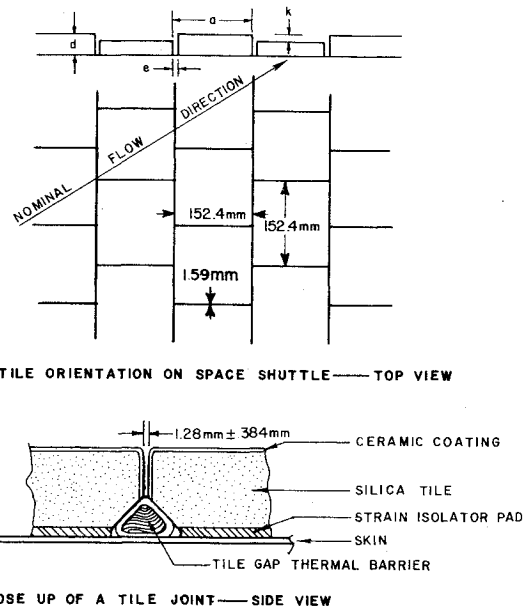

Fig. 1 Thermal protection system (TPS) tile layout for the space shuttle orbiter.

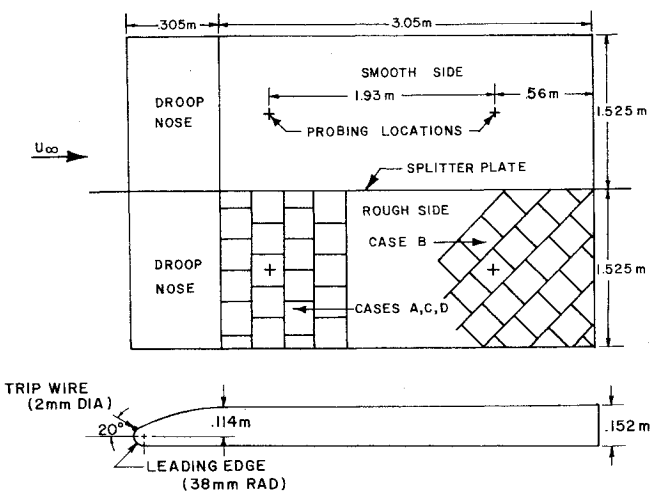

Fig. 2 Experimental apparatus for drag measurements of the TPS tiles.

The test plate was divided by a splitter plate which ran from front to rear to form two separate test areas. On one side of the splitter plate a smooth surface was simulated by covering it with Formica. This side served as a reference condition. The other half of the plate was used to hold 152.4 × 152.4 mm tiles in several different arrays.

Initial testing of the plate involved the use of surface tufts at $U_\infty = 28$ m/sec. The tufts indicated different stall patterns over the rough side compared to the smooth. In fact, the rough side demonstrated a stall angle several degrees higher than the smooth. This behavior was attributed to differing boundary-layer characteristics over the two sides. To correct this a 1.5 mm wire was attached about 20° from the leading edge, spanning the entire plate. The wire had the effect of raising the stall angle of both sides, as well as promoting a sharp stall characteristic with angle of attack. This change was credited to early transition of the boundary layer to turbulent flow. The data for skin friction indicated this to be the case except for the lowest speed ($U_\infty = 18.4$ m/sec). The test plate and the various configurations tested are illustrated in Fig. 2 and defined as follows: case A) 1.6 mm gaps normal to the flow direction, no steps; case B) 1.6 mm gaps 45° to the flow direction, no steps; case C) 1.6 mm gaps normal to the flow, 1.6 mm steps up and down; and case D) 1.6 mm gaps normal to the flow, 3.2 mm steps up and down.

Skin friction measurements were made by three indirect methods: 1) Preston tube,[1] 2) Clauser log-law method,[2] and 3) momentum integral. Of these, the Preston tube is valuable only for smooth walls, but served to monitor the smooth side skin friction for all pressure gradients. The Clauser method, although theoretically adequate for rough walls, proved unreliable. Thus, the momentum-integral method was employed for the rough side. The momentum-integral formulation for the friction coefficient is

$$C_f = \{2(d\theta/dx) + 2\theta[(H+2)/U_e](dU_e/dx)\} \quad (1)$$

Measurements of the velocity profile were used to determine θ and H at the probing stations. The values of U_e and dU_e/dx were determined from the 20 pressure static taps. Thus, values of $\bar{C}_f$, the average skin friction coefficient, could be obtained approximately by integrating Eq. (1)

$$\bar{C}_f = \frac{1}{\Delta x}\int_{x_1}^{x_2} C_f dx = 2\frac{(\theta_2-\theta_1)}{(x_2-x_1)} + 2\frac{\bar{\theta}(H+2)}{(x_2-x_1)}\int_{U_{e1}}^{U_{e2}}\frac{dU_e}{U_e} \quad (2)$$

The bars over certain terms in the above expression indicate averaging between x_1 and x_2 assuming normal Reynolds number behavior over the range.

For the case of zero pressure gradient, Eq. (2) reduces to

$$\bar{C}_f = 2(\theta_2-\theta_1)/(x_2-x_1) \quad (3)$$

Results

The measurements made by the three methods mentioned earlier provided some interesting observations on the TPS tile roughness effects on skin fricition. The results of the study are compared to accepted formulas for calculating skin friction for turbulent boundary layers over smooth walls.[3] It is useful first to compare the flow over the wind-tunnel plate to a flat plate. A typical example of the pressure distribution is given in Fig. 3. Here, the smooth side values are compared with case C at several angles of attack. Notice thay beyond $x/L = 0.25$, the pressure gradient varies rather evenly for the smooth side, yet is oscillatory over the rough side. The oscillations result because of the alternating raised and lowered tiles. The surface static pressure taps were located in the center of each tile in line from front to rear. For $\alpha = 0°$, the pressure gradient beyond $x/l = 0.25$ is very slight and thus approximates the flat plate case. Figure 4 presents the variation of the pressure coefficient for the nominal zero pressure gradient case. The oscillations in the static surface pressures increase markedly as the step size increases. These excursions in pressure coefficient would be typical of those expected on the space shuttle surface because of misalignment of the tiles.

In addition to the 20 static pressure ports, 5 Preston tubes were employed on each side of the plate. The Preston tube is valuable for smooth surfaces in pressure gradients. To illustrate their usefulness, Fig. 5 presents the results for local skin friction with respect to position for several angles of attack. The Preston-tube data are in good agreement with the Ludweig-Tillman[4] formula for skin friction, even for pressure gradients. The skin friction is seen to decrease as the pressure gradient becomes less favorable. When Preston tubes were used on the rough side, the indicated value of C_f decreased. This is not correct and occurred because the tubes were in the wake of the roughness.

The momentum-integral method relies on the measurment of the change in momentum in the boundary layer from one station to another. Any loss in momentum results in a surface force or the pressure drag over the roughness elements. The surface force may be due to a distributed shear stress or the drag over roughness elements. Using this method, the average skin friction coefficient between stations $\bar{C}_f$ is computed, as

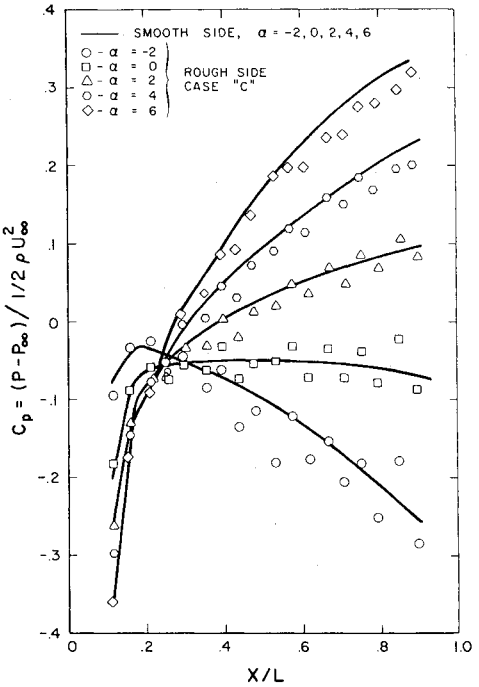

Fig. 3 Pressure distributions for case C as a function of angle of attack.

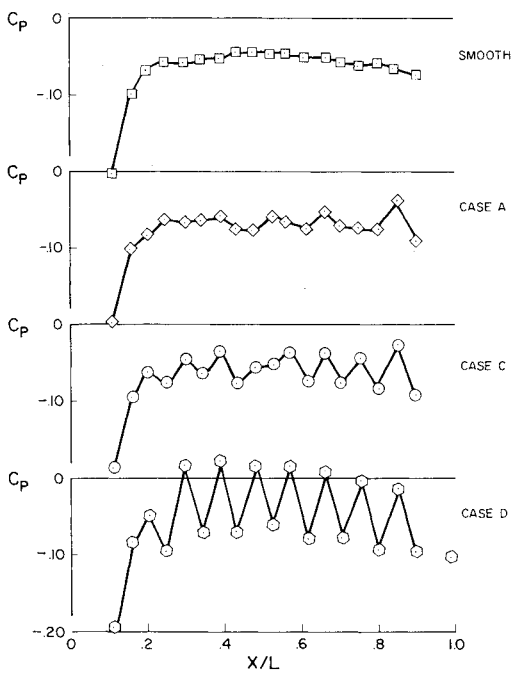

Fig. 4 Pressure distributions for the various cases at zero angle of attack.

opposed to the local values C_f. Thus, the momentum integral method does not rely on fitting a slope to local experimental data, but on the difference in the integrals of momentum at two planes.

Since the plate had no roughness on the droop nose and pressure gradients were not evaluated there, it was necessary to establish a virtual origin of the rough turbulent boundary layer which developed over the test plate. This was accomplished by assuming the form of growth of momentum thickness over the rough turbulent portion to be

$$\theta = G(Re_{x'})^{6/7} \tag{4}$$

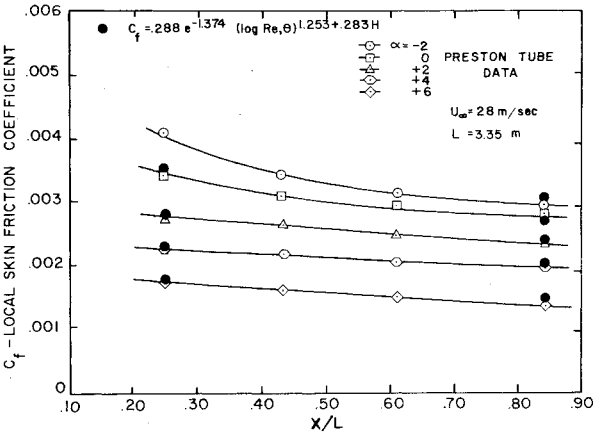

Fig. 5 Preston-tube skin-friction measurement for the smooth side.

where

$$x' = x - x_0' \tag{5}$$

Applying Eq. (3) at x_1 and x_2 where values of θ_1 and θ_2 where measured, the unknown constant G for a rough-wall boundary layer could be eliminated, and the virtual origin x_0' could be estimated. This procedure does not effect $x_2 - x_1$; however, it does determine a reference length $\bar{x}$ for a Reynolds number.

$$\bar{x} = [(x_2 - x_0') + (x_1 - x_0')]/2 = (x_2 + x_1)/2 - x_0' \tag{6}$$

Thus, a measured value of $\bar{C}_f$ applies at $\bar{x}$ and represents the average local skin friction expected over the distance, $x_2 - x_1$.

Figure 6 presents the average skin friction for the various cases as a function of angle of attack, the results are primarily for the momentum-integral method; however, an integrated Preston-tube result for a smooth surface is included for comparison. The cases with large roughness do not follow the same pattern with angle of attack as the relatively smooth cases. The Preston-tube data compare well with the momentum-integral method for all angles of attack if the wall is smooth.

Figure 7 summarizes the results of the study on TPS-type roughness for near zero pressure gradient. In the plot, there are several comparisons of importance. This plot presents, over a Reynolds number range from 1×10^6 to 8×10^6, the average drag coefficient of full-scale TPS tiles for the 4 cases compared with the smooth side. The experimental results are compared with the semiempirical method of Hoerner[5] for skin friction estimation. The solid symbols represent data corrected for a laminar flow condition which existed for the first 0.3 m of the curved nose section at the lowest tunnel speed ($U_\infty \simeq 18.4$ m/sec). The trip wire employed was apparently ineffective in producing transition at low velocities. Each case at this velocity exhibited a departure from the expected turbulent correlation. Therefore, the smooth side skin friction was adjusted upward to fit a curve through the higher Reynolds number data. This increment then was applied to the other lowest speed cases.

Analysis

The results indicate that the primary contribution to the skin-friction drag is from the steps for zero and nonzero pressure gradients. However, there is a recognizable trend towards increased drag due to slots and gaps. However, very slight misalignment of the tile surfaces in cases A and B could account for a portion of their drag. Thus, the analysis of the steps both forward and rear facing is the most significant task.

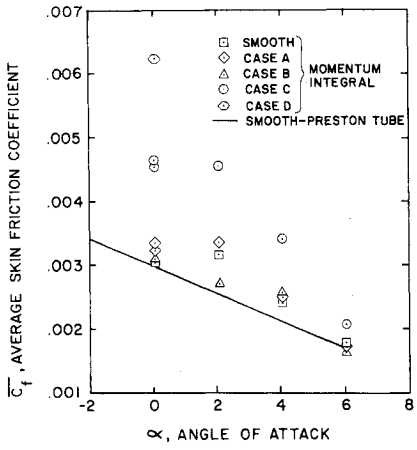

Fig. 6 Variation in average skin-friction coefficient with angle of attack.

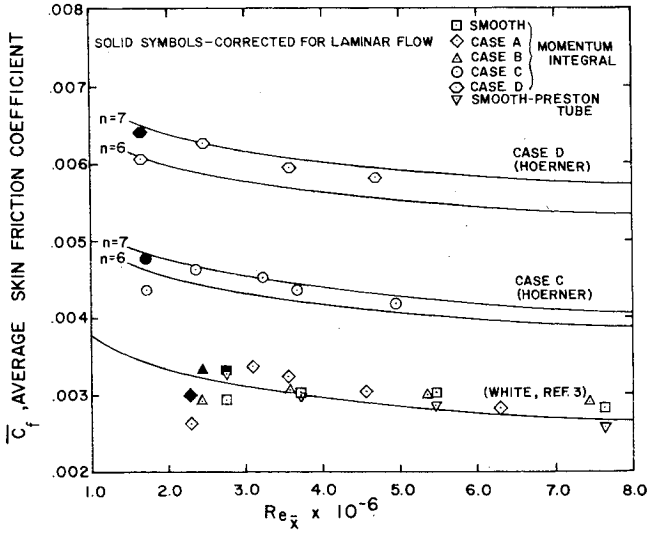

Fig. 7 Variation in average skin-friction coefficient with Reynolds number at zero angle of attack.

Method 1

The analysis of the contribution of the tiles to the skin-friction coefficient can proceed in several directions. Historically, the method of Hoerner[5] often is used in estimation the drag of isolated protuberances for aircraft. If the roughness elements are spaced greatly, they may be treated as additive components to the smooth wall skin friction. Thus, the sum of the drags of the roughness elements can be distributed over the surface and added to skin friction for a smooth wall. This procedure is outlined by Hoerner for a power-law formulation of the velocity profile. Similar procedures have been developed for a log-law profile.

$$C_f = C_{f,R} + C_{f,S} \tag{7}$$

In the present case, the roughness elements are of three types.

$$C_{f,R} = C_{f,\text{step}} + C_{f,\text{gap}} + C_{f,\text{slot}} \tag{8}$$

Since the area occupied by the roughness elements is fairly small (1:24) one of the correlations used to estimate the smooth-wall skin-friction coefficient can be employed. Based upon the measurements of the smooth side of the test plate, the correlation of White[3] appears best to fit the data

$$C_{f,S} = 0.455/[\ln^2(.06Re_x)] \tag{9}$$

Table 1 Element drag properties

Type	C_D	Basis	Area
Forward step	0.40	q_{eff} for k	$k \times a$
Backward step	0.22	q_{eff} for k	$k \times a$
Slot	0.284	q_{eff} for $k=e$	$k \times e$
Gap ($d/e > 0.7$)	0.014	q_{eff} for $k=0.7e$	$a \times e$

It is known, of course, that the roughness itself may act to increase the skin friction downstream of a roughness element where a new internal layer develops.

The procedure for determining $C_{f,R}$ employs the independent drag coefficient of the various roughness elements (the drag coefficient referenced to the effective dynamic pressure). Table 1 presents these coefficients for the present case and the basis upon which they are used in the analysis.

For the step, the equivalent local skin-friction coefficient for a reference freestream velocity can be calculated by

$$\overline{C}_{f,\text{step}} = \sum_{i=1}^{N} \left(\frac{k_i}{x_i}\right) C_{D,i} \frac{q_{eff,i}}{q_{e,i}} \left(\frac{q_{e,i}}{q_\infty}\right) \tag{10}$$

For a flat plate, $q_e/q_\infty = 1$ and q_{eff} can be evaluated by integrating the assumed velocity profile over the appropriate k

$$\frac{q_{eff}}{q_e} = \frac{1}{k}\int_o^k \left(\frac{U}{U_e}\right)^2 dy = \frac{n}{n+2}\left(\frac{k}{\delta}\right)^{2/n} \tag{11}$$

where

$$u/u_e = (y/\delta)^{1/n} \tag{12}$$

The boundary-layer thickness correlates with Reynolds number and length

$$\delta = F\,Re_x^{-2/(n+3)}x \tag{13}$$

where F depends upon the Reynolds number range in question. Hoerner[5] recommends

$$q_{eff}/q_e = 0.75\,(k/\delta)^{1/3} \text{ and } \delta/x = 0.016 \tag{14}$$

This result is based upon a $n=6$ power law; hence, is valid for $Re_L \simeq 10^6$. It generally is recognized that $n=7$ or 9 for $10^6 < Re_L < 10^8$. Using $n=7$ and $Re_L = 1\times 10^7$ as more typical of the present experiments and more representative of the shuttle, the value of $F=0.381$ is appropriate. Therefore,

$$q_{eff}/q_e = 0.778(k/\delta)^{2/7} \text{ and } \delta/x = 0.0152 \tag{15}$$

The results of the Hoerner method employing $n=6$ and $n=7$ are seen in Fig. 7. Note that the $n=7$ curves more closely approximate the experimental evidence. The results for the effect of roughness on skin friction for the present tests should be correlatable in the form of

$$\overline{C}_f = \overline{C}_{f,S} + E\sum_{i=1}^{N} C_{D,i}\left(\frac{k_i}{\bar{x}}\right)^{(n+2)/n} \tag{17}$$

Figure 8 compares Eq. (17) to the experimental results.

Method 2

A more general analysis of the results would occur if the log-law of the wall were employed since questions regarding n and Reynolds number no longer need to be answered explicitly. Further, method 1 makes no allowance for the shift in velocity profile which occurs for rough surfaces

$$u/u^* = A\ln y\delta/\nu + B - \Delta U_1/u^* \tag{18}$$

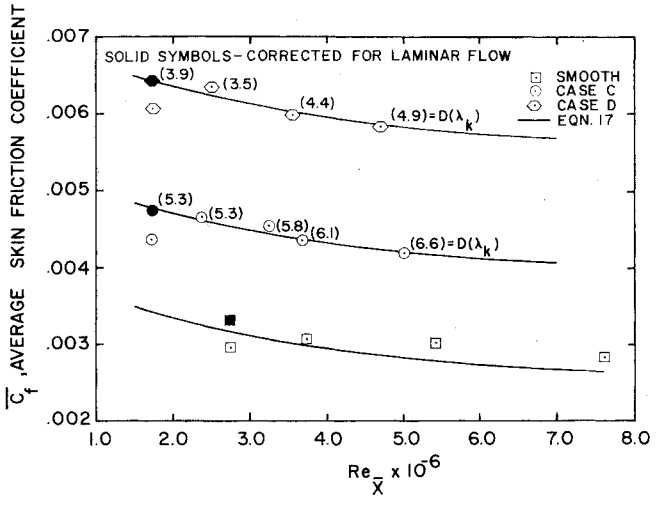

Fig. 8 Variation in average skin-friction coefficient compared to analytical correlations.

Applying this result at $y=\delta$ results in a skin-friction law for rough surfaces

$$(2/C_f)^{1/2} = A\ln(\delta^* U_e/\nu) + A\ln[(\delta^*/k)(C_f/2)^{1/2}] + B - \Delta U_1/u^* \quad (19)$$

or

$$(2/C_f)^{1/2} \simeq A\ln(\delta^* U_e/\nu) + C - \Delta U_1/u^* \quad (20)$$

where B and the second term on the right-hand side of Eq. (19) have been consolidated to form $C(C \simeq 4.8)$. This allows the use of δ^*, an integral property, in the correlation. The work of Clauser,[2] Dvorak,[6] and others[7,8] has shown that the effect of roughness of a given density λ (ratio of total surface area to the area occupied by the roughness) results in a uniform shift of the velocity profile for fully rough walls. In fact, Dvorak[6] has proposed a correlation for $\Delta U_1/u^*$ which includes the effects of λ for square rods

$$\Delta U_1/u^* = 2.44\ln(ku^*/\nu) + D(\lambda) \quad (21)$$

where $D(\lambda)$ varies with λ to form a maximum roughness effect at $\lambda = 4.68$. The friction law which follows from Eqs. (20) and (21) is

$$(2/C_f)^{1/2} = 2.44\ln[(\delta^*/k)(2/C_f)^{1/2}] + 4.8 - D(\lambda) \quad (22)$$

The form of Eq. (22) tends to minimize Reynolds number effects as viscosity and freestream velocity are removed from the correlation except in the manner in which they influence δ^*. Thus, for a given k and λ the predicted skin friction varies only slightly with Reynolds number. The correlation for $D(\lambda)$ given by Dvorak does correlate the data well for square rods whose long axis is normal to the flow.

$$D(\lambda) = 2.44\ln(u^*k/\nu) + 17.35[0.706\ln(\lambda) - 1] \quad (\lambda < 4.68) \quad (23)$$

$$D(\lambda) = 2.44\ln(u^*k/\nu) - 5.65[0.479\ln(\lambda) - 1] \quad (\lambda > 4.68) \quad (24)$$

Evidently below $\lambda = 4.68$, the flow tends to skim over the space between the roughness elements, thus reducing drag. As $\lambda \to 4.68$, the flow reattaches in the trough region between the elements, and as λ increases the pressure drag on each element increases, but, since the density is reduced, the total drag again reduces. For the tiles $\lambda = 2$, but this value would be for the skimming case, whereas significant reattachment in both the raised and lowered tiles should occur. A more recent interpretation of the roughness data has been provided by Simpson[9] and Furuya et al.[10] Their work indicates a new λ_k, defined as the ratio of the total surface area to the frontal area of the roughness, which correlates the data for all types of roughness elements more consistently. Simpson suggests simply replacing λ by λ_k in Eqs. (23) and (24). This modified parameter would show $\lambda_k = \infty$, 192, and 96 for cases *A*, *C*, and *D*, respectively. This interpretation shows more clearly that the tiles are in a region of reattachment following the infrequent steps. Based upon their work with a flat plate roughened by circular cylinders, Furuya et al.[10] have suggested a different correlation for $D(\lambda_k)$ *for* $\lambda_k > 4.68$.

$$D(\lambda_k) = -9.68[0.295\ln(\lambda_k) - 1] \quad (25)$$

Figure 8 notes the values of $D(\lambda_k)$ required to force the data to fit Eq. (22). The values of $D(\lambda_p)$ fit the values predicted by Eq. (25) closely. The correlation of Dvorak[6] [Eq. (24)] tends to underpredict the skin friction, whereas that of Furuya et al.[10] tends to be slightly conservative at the highest test Reynolds numbers.

The fact that there is a significant Reynolds number trend in the data indicates that the wall cannot be considered fully rough (ku^*/ν varies between 80 and 600 for these tests). Thus, the plate was evidently in the transitional roughness range which has yet to be explored fully.

Conclusions

For the space shuttle tile drag, the steps are the most significant feature. To a rough approximation, the drag increment beyond the smooth value is linearly proportional to the number and height of the vertical misalignments of the tiles. The magnitude of the drag increment due to roughness is relatively constant with Reynolds number over a range from 1 to 8×10^6. The results predicted by Hoerner are reasonable if a value for n appropriate to the Reynolds number is employed. Increased generality of the results should be obtained using the log-law formulation for skin friction on a rough surface. However, actually to use the results, a value for δ^* is required a priori although suitable estimation procedures could be devised. For the space shuttle orbiter the appropriate Reynolds number may be roughly one order of magnitude larger than the present experiments. This will be primarily because of an increased length scale for the orbiter, thus an increased boundary-layer thickness relative to a nominal step height should result. This should tend to reduce the roughness effects which would make an extension of the present results conservative in so far as method 2 is concerned. The method due to Hoerner[5] still should be appropriate if a proper power law (n) is chosen. Correlations for $\Delta U_1/u^*$ for rectangular roughness elements need to be determined; however, these will result only when a systematic study of the effects k, λ, and a variations is accomplished.

Acknowledgment

This work was sponsored by NASA, JSC under contract NAS9-11303.

References

[1] Preston, J., "The Determination of Turbulent Skin Friction by Means of Pitot Tubes," *Journal of the Royal Aeronautical Society*, Vol. 58, 1954, pp. 109-121.

[2] Clauser, F.H., "Turbulent Boundary Layers in Adverse Pressure Gradients," *Journal of Aeronautical Science*, Vol. 21, Feb. 1954, pp. 91-108.

[3] White, F.M., *Viscous Fluid Flow*, McGraw-Hill, New York, 1974, Chap. 6, p. 468.

[4] Ludweig, H. and Tillman, W., "Investigation of the Wall Shearing Stress in Turbulent Boundary Layers," NACA TM 1258, 1950.

[5] Hoerner, S., *Fluid-Dynamic Drag*, published by Author, Midland Park, N.J., 1965, Chap. 5.

[6]Dvorak, F.A., "Calculation of Turbulent Boundary Layers on Rough Surfaces in Pressure Gradient," *AIAA Journal,* Vol. 7, Sept. 1969, pp. 1752-1759.

[7]Betterman, D., "Contribution AL'etude De La Convection Forcee Turbulente Le Long Plaques Rogureses," *International Journal of Heat and Mass Transfer,* Vol. 9, 1966.

[8]Roberson, J.A., Bajwa, M., and Wright, S.J., "A General Theory for Flow in Rough Conduits," *Journal of Hydraulic Research,* Vol. 12, 1974, pp. 223-240.

[9]Simpson, R.L., "A Generalized Correlation of Roughness Density Effects on the Turbulent Boundary Layer," *AIAA Journal,* Vol. 11, Feb. 1973, pp. 242-244.

[10]Furuya, Y., Miyata, M., and Fujita, H., "Turbulent Boundary Layer and Flow Resistance on Plates Roughened by Wires," ASME Paper 76-FE-6, March 1976.